



# Acute desensitization of acetylcholine and endothelin-1 activated inward rectifier $K^+$ current in myocytes from the cardiac atrioventricular node

Stéphanie C.M. Choisy, Andrew F. James, Jules C. Hancox<sup>\*</sup>

School of Physiology & Pharmacology and Cardiovascular Research Laboratories, Medical Sciences Building, University of Bristol, Bristol BS8 1TD, UK

## ARTICLE INFO

### Article history:

Received 25 May 2012

Available online 5 June 2012

### Keywords:

Acetylcholine (ACh)

Atrioventricular node

AV node

AVN

Endothelin-1 (ET-1)

GIRK

$I_{KACH}$

Inward rectifier

Muscarinic potassium current

Tertiapin-Q

## ABSTRACT

The atrioventricular node (AVN) is a vital component of the pacemaker-conduction system of the heart, co-ordinating conduction of electrical excitation from cardiac atria to ventricles and acting as a secondary pacemaker. The electrical behaviour of the AVN is modulated by vagal activity *via* activation of muscarinic potassium current,  $I_{KACH}$ . However, it is not yet known if this response exhibits ‘fade’ or desensitization in the AVN, as established for the heart’s primary pacemaker – the sinoatrial node. In this study, acute activation of  $I_{KACH}$  in rabbit single AVN cells was investigated using whole-cell patch clamp at 37 °C. 0.1–1  $\mu$ M acetylcholine (ACh) rapidly activated a robust  $I_{KACH}$  in AVN myocytes during a descending voltage-ramp protocol. This response was inhibited by tertiapin-Q (TQ; 300 nM) and by the M2 muscarinic ACh receptor antagonist AFDX-116 (1  $\mu$ M). During sustained ACh exposure the elicited  $I_{KACH}$  exhibited bi-exponential fade ( $\tau_f$  of 2.0 s and  $\tau_s$  76.9 s at  $-120$  mV; 1  $\mu$ M ACh). 10 nM ET-1 elicited a current similar to  $I_{KACH}$ , which faded with a mono-exponential time-course ( $\tau$  of 52.6 s at  $-120$  mV). When ET-1 was applied following ACh, the ET-1 activated response was greatly attenuated, demonstrating that ACh could desensitize the response to ET-1. For neither ACh nor ET-1 was the rate of current fade dependent upon the initial response magnitude, which is inconsistent with  $K^+$  flux mediated changes in electrochemical driving force as the underlying mechanism. Collectively, these findings demonstrate that TQ sensitive inwardly rectifying  $K^+$  current in cardiac AVN cells, elicited by M2 muscarinic receptor or ET-1 receptor activation, exhibits fade due to rapid desensitization.

© 2012 Elsevier Inc. Open access under CC BY-NC-ND license.

## 1. Introduction

The atrioventricular node (AVN) of the heart is situated at the junction between the right atrium and ventricle [1] and is normally the only route by which electrical excitation can pass from atria to ventricles [2]. During atrial fibrillation the slow conduction properties of the AVN limit impulse transmission to the ventricles, thereby affording them some protection from an excessively fast ventricular rate [2,3]. The AVN also possesses pacemaker properties and can take over ventricular pacing should the primary pacemaker, the sinoatrial node (SAN), fail [2,4]. The electrophysiological properties of the intact AVN depend on both the anatomy and electrophysiology of the region [2,5] and the cellular electrophysiology of different sub-regions of the AVN depends on the interplay between a range of ion channel currents [6–8].

Vagal stimulation or application of acetylcholine (ACh) produces negative dromotropic and chronotropic effects on the AVN [2]. Activation of G-protein dependent, inwardly rectifying Kir3.1/3.4 channels is important to the cardiac actions of ACh [9,10]. Application of cholinergic agonists to small multicellular

AVN preparations or to single AVN cells activates an inwardly rectifying  $K^+$  current,  $I_{KACH}$  which decreases excitability [7,11–14], contributing to suppression of spontaneous activity [12,13] and, in perfused intact hearts, to AV conduction block [15]. In the SAN,  $I_{KACH}$  (likely carried by Kir3.1/3.4; [10]) contributes significantly to the negative chronotropic effect of ACh [16] and SAN  $I_{KACH}$  activation ‘fades’ in the continuous presence of ACh [17]. However, there is disagreement as to whether or not vagal responses of the AVN exhibit a ‘fade’ phenomenon. For example, in one study the negative dromotropic response of anaesthetised dogs to tonic vagal stimulation was reported to exhibit fade when the initial response to vagal stimulation was large [18], whilst in a separate study dromotropic effects of ACh in anaesthetised dogs were reported not to fade during maintained cholinergic activation [19]. On the other hand, vagal stimulation of rabbit isolated atrial preparations from which SAN and AVN responses were monitored simultaneously has been reported to produce membrane hyperpolarization that exhibited similar fade in both regions [20]. We have recently observed transient activation in isolated AVN myocytes of a tertiapin-Q sensitive inwardly rectifying  $I_{KACH}$ -like current by the peptide hormone ET-1 [21]. This raises the possibility that muscarinic activation of  $I_{KACH}$  in myocytes from the AVN is followed by fade/desensitization of the response. The present study was con-

<sup>\*</sup> Corresponding author. Fax: +44 1173312288.

E-mail address: [jules.hancox@bristol.ac.uk](mailto:jules.hancox@bristol.ac.uk) (J.C. Hancox).

ducted to test this proposition, using an established single AVN cell preparation from the rabbit heart [13].

## 2. Methods

### 2.1. Rabbit AVN cell isolation

Male White New-Zealand rabbits (~2.0–3.5 kg) were killed in accordance with the United Kingdom Home Office Animals Scientific Procedures Act (1986). Their hearts were rapidly excised and cells isolated from the entire atrioventricular nodal (AVN) region as described previously [13,22,23]. Isolated AVN cells were stored in Kraft-Brühe “KB” solution [13,24] at 4 °C until use.

### 2.2. Electrophysiological recording

Cells were placed in an experimental chamber (0.5 ml) mounted on the stage of an inverted microscope (Nikon Diaphot) and superfused with a normal Tyrode's solution, containing (in mM): NaCl 140, KCl 4, CaCl<sub>2</sub> 2, MgCl<sub>2</sub> 1, HEPES 5 and Glucose 10, (pH 7.4 with NaOH). ACh, ET-1 and other compounds were added to this solution. Patch-pipettes (Corning 7052 glass, AM Systems Inc., Sequim, WA, USA) were pulled using a P-97 Flaming/Brown micropipette puller (Sutter Instruments, Novato, CA, USA) and were filled with a pipette solution containing (in mM) [23,25]: KCl 110, NaCl 10, HEPES 10, MgCl<sub>2</sub> 0.4, and Glucose 5, K<sub>2</sub>ATP dihydrate 5, GTP-Tris salt 0.5, BAPTA 5, pH 7.1 with KOH. Recordings were made using an Axopatch 1D amplifier (Axon Instruments; now Molecular Devices, Sunnyvale, CA, USA). Pipette resistance was typically <3 MΩ; series resistance was typically compensated by ~60–80%. Under voltage clamp, membrane potential was held at –40 mV as this value corresponds to the zero current potential for rabbit AVN cells (e.g. [13,26]). Electrophysiological protocols were generated and data recorded using Clampex 8 (Axon Instruments; CA, USA). Repetitive application of a descending voltage ramp protocol (shown in the left panel of Fig. 1A) was used to survey rapidly current between +20 and –120 mV. A brief (50 ms) step from –40 to +20 mV preceded the descending ramp in the voltage protocol. The initial depolarizing step phase of the protocol elicited an L-type calcium current ( $I_{Ca,L}$ ), which was used as an independent marker of AVN cell responsiveness to ACh (and ET-1), as both receptor agonists inhibit AVN  $I_{Ca,L}$  (e.g. [12,13,21]).

### 2.3. Solutions and chemicals

Cells were superfused with experimental solutions at 35–37 °C (checked regularly using a hand-held thermocouple). ACh, ET-1 and other compounds were applied externally to the cell under study using a home-built, rapid solution exchange device capable of exchanging superfusate in <1 s [27]. ACh (Sigma–Aldrich Company Ltd., Dorset, UK) was used at 0.1 and 1 μM from a stock solution (1 or 10 mM) made each experimental day in distilled, deionized water. ET-1 (Sigma–Aldrich Company Ltd., Dorset, UK) was used at 10 nM from a stock solution of 100 μM prepared in 0.1% acetic acid. Tertiapin-Q (Tocris Bioscience, Bristol, UK) was prepared in deionised water and used at a final concentration of 300 nM in Tyrode's solution. AFDX-116 (Ascent Scientific, Bristol) was used at 1 μM from a stock solution made in DMSO. All drug stocks except ACh were aliquoted and stored at –20 °C.

### 2.4. Data analysis

Data were analysed and graphical plots produced using Clampfit 10.2 software (Molecular Devices Sunnyvale, CA, USA), Microsoft Excel (2003) and GraphPad Prism (v5; GraphPad Software

Inc., La Jolla, CA, USA). Data are presented as mean ± standard error of the mean (SEM). Statistical analysis was performed using Student's *t*-test, one-way ANOVA with a Bonferroni post hoc test. Values of '*p*' less than 0.05 were taken as significant.

## 3. Results and discussion

One micromolar of ACh was employed to elicit  $I_{KACH}$  in this study, as this concentration has been established to produce a robust activation of AVN cell  $I_{KACH}$  [7], leading to rapid membrane potential hyperpolarisation and quiescence in AVN cell and tissue preparations [12,13]. Fig. 1A (right panel) shows representative currents during the descending ramp phase of the command protocol plotted against voltage, obtained in normal Tyrode's solution and immediately following rapid application of ACh. One micromolar of ACh increased current across the entire range of measured voltages. In ACh the net current during the ramp exhibited marked inward rectification and reversed slightly negative to –80 mV. Fig. 1B shows the mean current density–voltage (*I*–*V*) relation for the maximal ACh-activated current,  $I_{KACH}$  (*n* = 6). The mean reversal potential ( $E_{rev}$ ) for this current was  $-85.5 \pm 0.6$  mV. In additional experiments,  $I_{KACH}$  was activated by a lower ACh concentration (0.1 μM); the current profile was similar to that produced by 1 μM ACh, but was of smaller magnitude. The M2 receptor is considered to be the predominant muscarinic receptor sub-type in mammalian heart [28]. When AVN cells were pre-treated with the M2 receptor inhibitor AFDX-116 (1 μM), the response to 1 μM ACh was largely abolished (Fig. 1C), demonstrating M2 receptor activation to be responsible for generation of AVN  $I_{KACH}$ . This is concordant with: (i) prior work on anaesthetised dogs in which AFDX-116 inhibited chronotropic and dromotropic responses to intracardiac vagal nerve stimulation [29]; (ii) the persistence of AV conduction block in response to intravenous ACh in mice deficient in M1-receptors [30], and (iii) presumed M2-receptor mediated conduction effects of propofol on guinea-pig hearts [31]. SAN  $I_{KACH}$  is sensitive to the bee venom toxin tertiapin [32,33]. To our knowledge, there are no similar data for AVN  $I_{KACH}$  *per se*, although ACh effects on guinea-pig atrio-ventricular conduction have been shown to be sensitive to tertiapin [15]. When we applied ACh to cells after exposure to tertiapin Q (300 nM),  $I_{KACH}$  was largely abolished (Fig. 1C). Collectively, the data in Fig. 1 demonstrate that rabbit AVN  $I_{KACH}$  is tertiapin-Q sensitive and involves ACh binding to M2 muscarinic receptors.

Fig. 2 shows the time-course of the effect of sustained exposure to 1 μM ACh. Fig. 2A and B show representative time-plots for current at two voltages (+20 and –120 mV) during the voltage ramp protocol. It is clear that at both voltages ACh application led to a maximal response within seconds of its application. However, in the maintained presence of ACh the current response declined over ~2 min, with an initial rapid decline followed by a slower second phase. In six experiments the peak response at –120 mV was  $-37.6 \pm 5.1$  pA/pF, whilst after 2 min of ACh application the response declined to an amplitude of  $-16.9 \pm 0.8$  pA/pF (*p* < 0.01). At +20 mV, the peak response amplitude was  $21.0 \pm 2.6$  pA/pF, declining to  $9.3 \pm 1.1$  pA/pF at 2 min of ACh application (*p* < 0.01). Thus, acute activation of AVN  $I_{KACH}$  exhibited rapid bi-phasic 'fade'. This was quantified by bi-exponential fitting of the decline of net current at each voltage; data from individual cells at each time-point were normalised to maximal current in ACh, and then pooled. Fits to the mean data are shown in Fig. 2C (at +20 mV) and 2D (at –120 mV). At –120 mV 62.2 ± 6.7% of the current decline was described by a time-constant ( $\tau_f$ ) of 2.0 s, whilst the remainder of the current decline was described by a time-constant ( $\tau_s$ ) of 76.9 s (see Fig. 2 legend for further numerical information). In contrast to the situation for  $I_{KACH}$ ,  $I_{Ca,L}$  elicited by the +20 mV

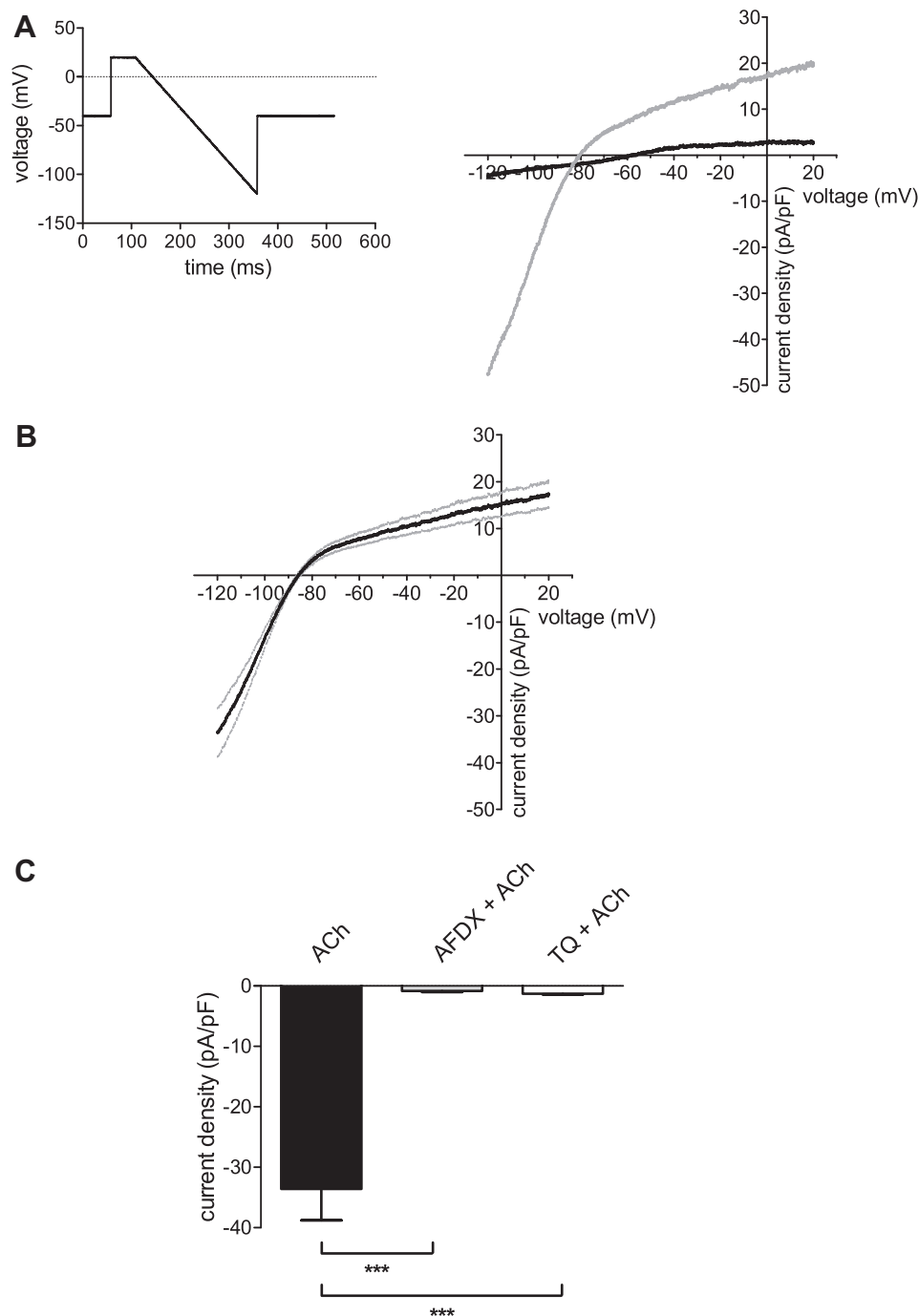


**Fig. 1.** Activation of AVN  $I_{KACH}$  and sensitivity to M2 receptor inhibition and tertiapin-Q (A) Left panel shows voltage protocol used: from a holding potential of  $-40$  mV, a step to  $+20$  mV for 50 ms preceded a descending voltage-ramp to  $-120$  mV over 250 ms. The start-to-start interval between successive applications of the protocol was 2 s. Right panel shows representative currents elicited in control (normal Tyrode's) solution (black trace) and immediately following rapid superfusion of  $1 \mu$ M ACh (grey trace). (B) Mean current-voltage ( $I$ - $V$ ) relation for current activated by  $1 \mu$ M ACh ( $n = 6$ ; obtained by digital subtraction of current in control from that in ACh and normalised to cell membrane capacitance). The black trace denotes the mean current values at each voltage, with grey traces indicating  $\pm$ SEM values. (C) Mean current-density (pA/pF) of the maximal  $I_{KACH}$  at  $-120$  mV ( $1 \mu$ M ACh sensitive current) in the presence of ACh alone (black bar;  $n = 6$ ), with  $1 \mu$ M of the M2 muscarinic receptor inhibitor AFDX-116 (grey bar;  $n = 5$ ), and in the presence of 300 nM of the GIRK channel inhibitor tertiapin-Q (white bar;  $n = 6$ ). Asterisks denote statistically significant differences (\*\* $p < 0.001$ ).

voltage step phase of the voltage protocol decreased monotonically with  $1 \mu$ M ACh application (not shown), declining by  $41.7 \pm 6.0\%$  ( $n = 6$ ) of its initial amplitude by  $\sim 2$  min following the peak  $I_{KACH}$  response. The biphasic nature of the fade of AVN cell  $I_{KACH}$  in this study correlates qualitatively with a reported biphasic decline of hyperpolarising response of the rabbit intact AVN to trains of vagal nerve stimuli [20], although in absolute terms the time-course of the observed fade of the intact node membrane potential response

was faster than that seen here [20]. Differences in time-course of response decline between that study and this one are likely to be accounted for by the different preparations used (intact tissue versus isolated cell) and mode and duration of vagal activation (vagal nerve stimulation versus sustained superfusion of ACh).

Recent data from experiments conducted using voltage-step protocols have shown that ET-1, acting through the  $ET_A$  receptor, transiently activates a tertiapin-Q sensitive  $K^+$  current that resem-

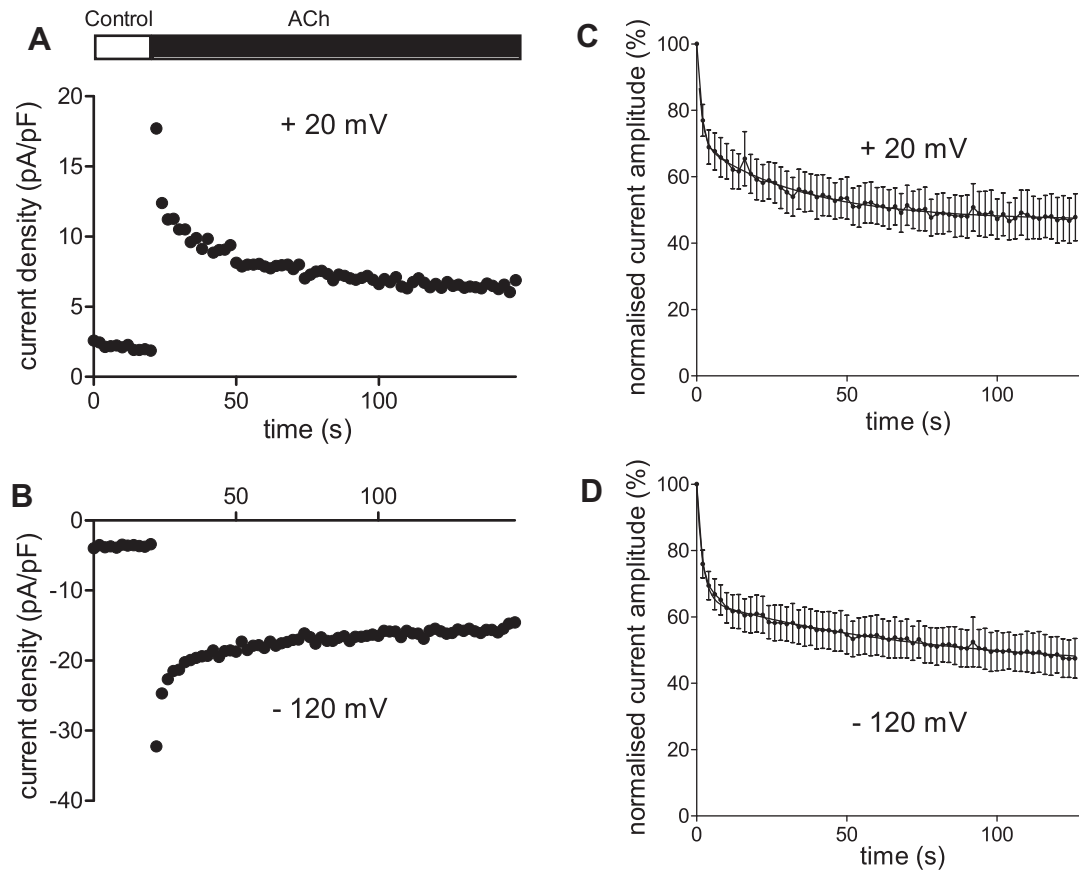


**Fig. 2.** Time-course of fade of the ACh response. (A and B) show representative continuous time-plots of current at +20 mV (A) and –120 mV (B) before and during exposure to 1  $\mu$ M ACh. Time of ACh application is denoted by the horizontal bar in panel A. (C and D) show mean data-plots ( $n = 6$ ) in which for each cell the net current amplitude was normalised to the maximum response in the presence of ACh at +20 mV (C) and –120 mV (D). Data were fitted by a two-phase decay equation. At +20 mV  $56.1 \pm 8.8\%$  of the declining current was characterised by a fast rate of decline ( $K_{\text{fast}}$  of  $0.67 \pm 0.42 \text{ s}^{-1}$  (equivalent to a  $\tau_f$  of 1.5 s) whilst the remainder of current decline was characterised by a slow rate of decline ( $K_{\text{slow}}$  of  $0.029 \pm 0.012 \text{ s}^{-1}$  (equivalent to a  $\tau_s$  of 34.5 s). At –120 mV  $62.2 \pm 6.7\%$  of current decline was characterised by a  $K_{\text{fast}}$  of  $0.50 \pm 0.20 \text{ s}^{-1}$  ( $p > 0.7$  versus +20 mV; equivalent to a  $\tau_f$  of 2 s), whilst the remainder of current decline was characterised by a  $K_{\text{slow}}$  of  $0.013 \pm 0.011 \text{ s}^{-1}$  ( $p > 0.3$ ; equivalent to a  $\tau_s$  of 76.9 s).

bles  $I_{\text{KACH}}$  [21]. Consequently, for comparison with our observations on  $I_{\text{KACH}}$ , we conducted experiments with ET-1 using the same voltage protocol used to study ACh. Fig. 3A shows the time-course of current activation by ET-1 at +20 and –120 mV during the voltage ramp protocol. At both voltages ET-1 application led to a maximal response within seconds of its application (mean  $I$ – $V$  data for peak ET-1 activated current are shown in Fig. 3B, showing the response to be very similar to that to ACh (Fig. 1B), though of smaller magnitude). Also similar to ACh, in the maintained presence of ET-1 the response magnitude declined over a 2–3 min recording period. This is shown for an individual experiment in Fig. 3A and in Fig. 3C and D for mean data (normalised to maximal response amplitude as for ACh in Fig. 2). The rate of decline of the ET-1 response could be described satisfactorily by a single exponential function, with time-constant values of 55.5 and 52.6 s respectively at +20 and –120 mV. As reported recently [21], 10 nM ET-1 also produced a monotonic decrease in the amplitude  $I_{\text{Ca,L}}$  elicited by the +20 mV voltage step (declining by  $69.7 \pm 3.3\%$  ( $n = 6$ ) at  $\sim 2$  min of exposure).

Acute desensitization of  $I_{\text{KACH}}$  in rat atrial myocytes has been proposed to depend on  $\text{K}^+$  ion flow and to arise due to an acute reduction in electrochemical driving force for  $\text{K}^+$  ion flow rather than from changes to receptor-coupled signalling [34]. If such an explanation applies to AVN cells, then the magnitude of peak response to ACh (representing an index of  $\text{K}^+$  flux) might be expected to determine the rate of subsequent current decline. Fig. 4A and B respectively show plots of the  $\tau_f$  and  $\tau_s$  of decline of ACh responses

against the initial peak magnitude of the current response, incorporating data with both 0.1 and 1  $\mu$ M ACh (respectively, open and filled symbols). There was no significant correlation between either time constant and the initial response amplitude ( $r$  of 0.0 for  $\tau_f$  and  $-0.4$  for  $\tau_s$ , with respective  $p$  values of 1.0 and 0.2). Fig. 4C shows similar data for ET-1, demonstrating little correlation between fade time constant and initial response amplitude ( $r$  of 0.09,  $p$  of 0.9). Thus, regardless of the receptor system by which  $I_{\text{KACH}}$  was activated, there was no relation between the rate of fade and the magnitude of  $\text{K}^+$  flux. In addition, were a change in the electrochemical driving force for  $\text{K}^+$  flow to result from activation of AVN  $I_{\text{KACH}}$ , this might be expected to be reflected in a positive shift in the reversal potential for the current during continued application of the agonist. Fig. 4D shows plots of  $E_{\text{rev}}$  for the 1  $\mu$ M ACh-activated current at the time-point of peak response to ACh and at 6 s after the initial peak (at which time-point any initial decline would have been attributable to the fast component of current fade) and after 2 min of ACh application (by which time-point both fast and slow fade would have occurred). The values obtained at the three time points did not differ significantly, indicating that statistically significant changes in electrochemical driving force (and thereby  $E_{\text{rev}}$ ) had not occurred ( $p > 0.1$ ). In this regard our results are similar to those from a prior study of guinea-pig atrial myocytes, in which biphasic fade of  $I_{\text{KACH}}$  occurred with no alteration in  $E_{\text{rev}}$  for the current [35]. Thus, it can be concluded that, in contrast to the mechanism proposed for rat atrial myocytes by Bender et al. [34], the fade of  $I_{\text{KACH}}$  in AVN cells does not depend

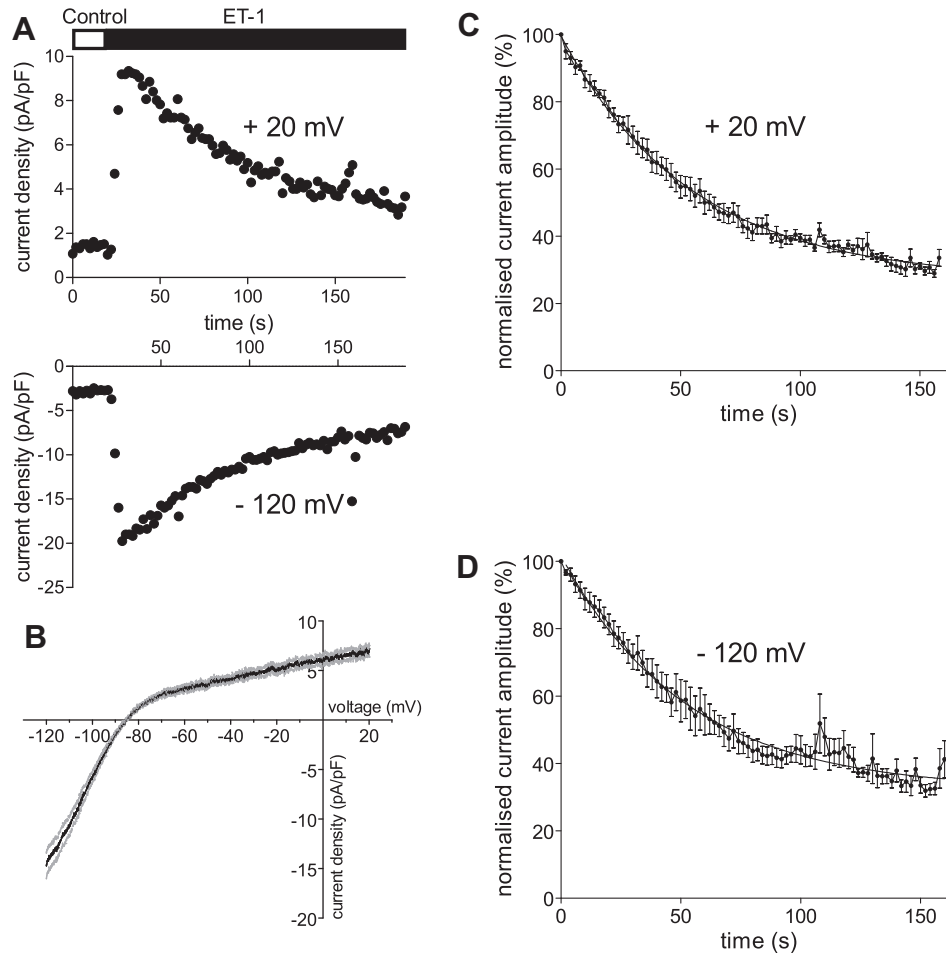


**Fig. 3.** Fade of ET-1 activated K<sup>+</sup> current. (A) shows representative continuous time-plots of current at +20 mV (upper panel) and –120 mV (lower panel) before and during exposure to 10 nM ET-1. Time of ET-1 application is denoted by the horizontal bar in upper panel. Voltage protocol same as Fig. 1A. (B) shows mean current density–voltage relation for ET-1 activated current ( $n = 6$ ). (C, D) show mean data indicating time-course of decline of response to ET-1 at +20 mV (C) and –120 mV (D). Data were normalised as for ACh in Fig. 2. The fade in response exhibited monophasic decline with rate constants of  $0.018 \pm 0.001 \text{ s}^{-1}$  and  $0.019 \pm 0.001 \text{ s}^{-1}$  for +20 and –120 mV, respectively ( $p > 0.4$ ; equivalent to  $\tau$  values of 55.5 and 52.6 s).

on K<sup>+</sup> ion flow and represents genuine desensitization of the response to ACh.

In a final set of experiments, we investigated whether or not ACh was able to cause desensitization of the response to ET-1. In these experiments 1  $\mu\text{M}$  ACh was applied and after the response had exhibited considerable fade (with at least two minutes of ACh exposure), ET-1 was then rapidly applied in the maintained presence of ACh. Fig. 4E shows representative traces of the ACh-sensitive current at the peak of the ACh response (black trace) and after 2 min in the presence of ACh (light grey trace). Also superimposed is the peak ET-1-sensitive current following subsequent ET-1 application (dark grey trace); it is notable that under these conditions relatively little additional current was activated by ET-1. Fig. 4F shows the mean current density at –120 mV of ACh-activated and ET-1 activated current (when each agonist was applied separately), together with the mean ET-1 activated current density for cells receiving prior ACh exposure. The small size of the ET-1 activated current following exposure to ACh in comparison to the response to ET-1 alone indicates that ACh and ET-1 responses are not simply additive. Furthermore, once the ACh response had faded, the affected channels appeared to be relatively unresponsive to ET-1. Thus, it can be concluded that ACh causes desensitization not only of the ACh-sensitive K<sup>+</sup> current but also of the ET-1-sensitive K<sup>+</sup> current (this was not the case for  $I_{\text{Ca,L}}$ , which was still able to respond to ET-1 with a

$66.0 \pm 8.0\%$  ( $n = 6$ ) decline, following prior ACh exposure (data not shown; not significantly different from extent of reduction without ACh pre-treatment;  $p > 0.6$ ). This observation suggests that despite working through different receptors, ET-1 and ACh share pathways of action downstream from the receptors and likely elicited their responses by acting on the same pool of K<sup>+</sup> channels; furthermore once the ACh response had faded, the affected channels appeared to be relatively unresponsive to ET-1. To our knowledge, this may constitute the first report for any region of the heart of cross-desensitization by ACh of the cardiac G-protein-dependent inwardly rectifying current activated by an agonist of a distinct receptor.

In conclusion, this study establishes that both M2 muscarinic receptor and ET-1 activated “ $I_{\text{KACH}}$ ” in AVN cells exhibit marked fade during continuous exposure to ACh and ET-1. The two different receptor agonists appear to act on the same underlying K<sup>+</sup> channel pool. Acute fade of  $I_{\text{KACH}}$  is not explicable as a consequence of K<sup>+</sup> flux mediated alterations to electrochemical K<sup>+</sup> driving force. Rather it is likely to involve desensitization of the receptor/signaling pathway. Involvement of a receptor-linked mechanism is also consistent with differences in the time-course of fade of 10 nM ET-1 and 1  $\mu\text{M}$  ACh responses; such differences would not be expected from a mechanism depending purely on K<sup>+</sup> ion flux. Muscarinic receptor-mediated inhibition of AVN basal  $I_{\text{Ca,L}}$  has been proposed to involve suppression of cAMP synthesis [36] or nitric-oxide mod-



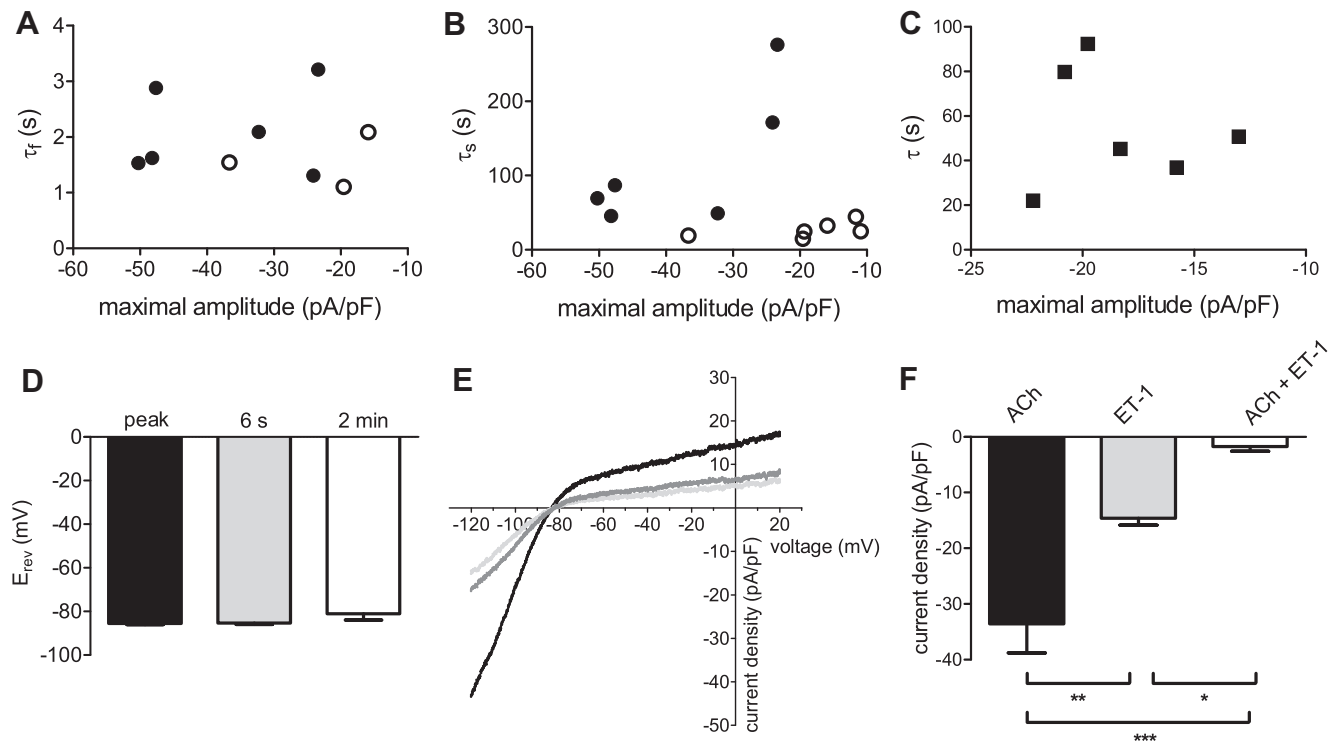


**Fig. 4.** Relationship between K<sup>+</sup> current response magnitude and decline rate, and effect of combined ACh and ET-1 application. (A and B) Plots of time constants of current fade (A:  $\tau_{fast}$  ( $\tau_f$ ); B:  $\tau_{slow}$  ( $\tau_s$ )) against magnitude of initial response to 1  $\mu$ M ACh ( $n = 6$ ; filled circles). Open circles show data for 0.1  $\mu$ M ACh. For this concentration of ACh 3 cells exhibited biphasic decay and 3 cells monophasic decay; for the latter, the single  $\tau$  values are plotted in B. (C) Plot of time constant of current fade against magnitude of initial response to 10 nM ET-1 ( $n = 6$ ; filled circles). (A)–(C) time-course measured for responses at  $-120$  mV. (D) Plot of  $E_{rev}$  for  $I_{KACH}$  activated by 1  $\mu$ M ACh at the initial peak of the response (black bar), at 6 s following the maximal response (grey bar) and at 2 min following maximal response (open bar). There was no significant difference in  $E_{rev}$  values at the different time-points ( $n = 6$ ;  $p > 0.1$ ). (E and F) Effects of 10 nM ET-1 following prior exposure to 1  $\mu$ M ACh. (E) shows representative currents (plotted as current density against voltage) for responses in the same cell to 1  $\mu$ M ACh ( $I_{KACH}$ ) measured as ACh-activated current at maximal response (black trace) and 2 min after the maximal response (light grey trace). The dark grey trace shows maximal current in 10 nM ET-1 (plotted as ET-1 activated current compared to control) following 2 min exposure to ACh. In the concomitant presence of ACh, ET-1 elicited little additional current. (F) Maximal current densities for current at  $-120$  mV for ACh-activated current (black bar;  $n = 6$ ), ET-1 (grey bar;  $n = 6$ ), and the ET-1 difference current (ET-1 minus ACh) when ET-1 was applied following fade of the ACh response. Asterisks denote statistical significance (\* $p < 0.05$ , \*\* $p < 0.01$  and \*\*\* $p < 0.001$ ).

ulation of cGMP-stimulated phosphodiesterase [14]; the lack of fade of the response of  $I_{Ca,L}$  to ACh in the present study suggests that these pathways are unlikely to be involved in AVN  $I_{KACH}$  fade/desensitization. Cardiac muscarinic K<sup>+</sup> current desensitization has been suggested to involve mechanisms involving G protein-coupled receptor kinase (GRK2),  $\beta$  arrestin and M2 receptor internalisation (e.g. [37–40]). Further work is required to elucidate the contributions of such mechanisms to AVN cell  $I_{KACH}$  desensitization. However, the fact that in our experiments the inhibitory effects of ACh and ET-1 on  $I_{Ca,L}$  were sustained in the same cells in which  $I_{KACH}$  fade occurred, suggests either that rapid receptor internalisation was not responsible for desensitization of the AVN cell K<sup>+</sup> current response in our experiments, or that the M2 receptors coupled to channels modulating  $I_{Ca,L}$  and  $I_{KACH}$  reside in different pools. Rapid cross-desensitization of ET-1 activated K<sup>+</sup> current by prior ACh exposure is likely to occur down-stream of the ET-1 receptor itself, but could feasibly involve GRK2 linked desensitization of those ET<sub>A</sub> receptors coupled to K<sup>+</sup> channels [41,42]. Fade of  $I_{KACH}$  may provide a mechanism for physiological adaptation of the AVN to cholinergic stimulation [20,43]. Further investigation of this phenomenon and of the mechanism(s) underlying desensitization is now warranted.

#### Acknowledgments

The authors thank the British Heart Foundation for funding (PG/08/104; PG/11/97), Mrs Lesley Arberry for technical assistance and

Dr Hongwei Cheng and Ms Hanne Gadeberg for help with cell isolation.

#### References

- [1] S. Tawara, Das Reizleitungssystem des Säugetierherzens, Fischer Jena, Germany, 1906.
- [2] F.L. Meijler, M.J. Janse, Morphology and electrophysiology of the mammalian atrioventricular node, *Physiol. Rev.* 68 (1988) 608–647.
- [3] R. Langendorf, A. Pick, Concealed conduction. Further evaluation of a fundamental aspect of propagation of the cardiac impulse, *Circulation* 13 (1956) 380–399.
- [4] R. Childers, The AV node: Normal and abnormal physiology, *Progress in Cardiovascular Diseases* XIX (1977) 361–381.
- [5] I.R. Efimov, V.P. Nikolski, F. Rothenberg, I.D. Greener, J. Li, H. Dobrzynski, M. Boyett, Structure–function relationship in the AV junction, *Anat. Rec. A Discov. Mol. Cell Evol. Biol.* 280 (2004) 952–965.
- [6] A.A. Munk, R.A. Adjeiman, J. Zhao, A. Ogbaghebril, A. Shrier, Electrophysiological properties of morphologically distinct cells isolated from the rabbit atrioventricular node, *J. Physiol.* 493.3 (1996) 801–818.
- [7] J.C. Hancox, K.H. Yuill, J.S. Mitcheson, M.K. Convery, Progress and gaps in understanding the electrophysiological properties of morphologically normal cells from the cardiac atrioventricular node, *Int. J. Bifurcation Chaos* 13 (2003) 3675–3691.
- [8] S. Inada, J.C. Hancox, H. Zhang, M.R. Boyett, One-dimensional mathematical model of the atrioventricular node including atrio-nodal, nodal, and nodal-his cells, *Biophys. J.* 97 (2009) 2117–2127.
- [9] H. Hibino, A. Inanobe, K. Furutani, S. Murakami, I. Findlay, Y. Kurachi, Inwardly rectifying potassium channels: their structure, function, and physiological roles, *Physiol. Rev.* 90 (2010) 291–366.
- [10] M.E. Mangoni, J. Nargeot, Genesis and regulation of the heart automaticity, *Physiol. Rev.* 88 (2008) 919–982.

- [11] B. Sakmann, A. Noma, W. Trautwein, Acetylcholine activation of single muscarinic K<sup>+</sup> channels in isolated pacemaker cells of the mammalian heart, *Nature* 303 (1983) 250–253.
- [12] M. Nishimura, Y. Habuchi, S. Hiromasa, Y. Watanabe, Ionic basis of depressed automaticity and conduction by acetylcholine in rabbit AV node, *Am. J. Physiol.* 255 (1988) H7–H14.
- [13] J.C. Hancox, A.J. Levi, C.O. Lee, P. Heap, A method for isolating rabbit atrioventricular node myocytes which retain normal morphology and function, *Am. J. Physiol.* 265 (1993) H755–H766.
- [14] X. Han, L. Kobzik, J.L. Balligand, R.A. Kelly, T.W. Smith, Nitric oxide synthase (NOS3)-mediated cholinergic modulation of Ca<sup>2+</sup> current in adult rabbit atrioventricular nodal cells, *Circ. Res.* 78 (1996) 998–1008.
- [15] M.D. Drici, S. Diochot, C. Terrenoire, G. Romey, M. Lazdunski, The bee venom tertiapin underlines the role of I<sub>KACH</sub> in acetylcholine-induced atrioventricular blocks, *Br. J. Pharmacol.* 131 (2000) 569–577.
- [16] M.R. Boyett, I. Kodama, H. Honjo, A. Arai, R. Suzuki, J. Toyama, Ionic basis of the chronotropic effect of acetylcholine on the rabbit sinoatrial node, *Cardiovas. Res.* 29 (1995) 867–878.
- [17] H. Honjo, I. Kodama, W.J. Zang, M.R. Boyett, Desensitization to acetylcholine in single sinoatrial node cells isolated from rabbit hearts, *Am. J. Physiol.* 263 (1992) H1779–H1789.
- [18] P. Martin, Secondary AV conduction responses during tonic vagal stimulation, *Am. J. Physiol.* 245 (1983) H584–H591.
- [19] J.M. Loeb, J.M. deTarnowsky, Maintained prolongation of AV conduction time by acetylcholine, *Eur. J. Pharmacol.* 100 (1984) 351–356.
- [20] J.J. Salata, J. Jalife, “Fade” of hyperpolarizing responses to vagal stimulation at the sinoatrial and atrioventricular nodes of the rabbit heart, *Circ. Res.* 56 (1985) 718–727.
- [21] S.C. Choisy, H. Cheng, G.L. Smith, A.F. James, J.C. Hancox, Modulation by endothelin-1 of spontaneous activity and membrane currents of atrioventricular node myocytes from the rabbit heart, *PLoS One* 7 (2012) e33448.
- [22] J.C. Hancox, A.J. Levi, The hyperpolarisation-activated current, I<sub>h</sub> is not required for pacemaking in single cells from the rabbit atrioventricular node, *Pflügers Arch.* 427 (1994) 121–128.
- [23] H. Cheng, G.L. Smith, C.H. Orchard, J.C. Hancox, Acidosis inhibits spontaneous activity and membrane currents in myocytes isolated from the rabbit atrioventricular node, *J. Mol. Cell. Cardiol.* 46 (2009) 75–85.
- [24] G. Isenberg, U. Klockner, Calcium tolerant ventricular myocytes prepared by incubation in a “KB medium”, *Pflügers Arch.* 395 (1982) 6–18.
- [25] H. Cheng, G.L. Smith, J.C. Hancox, C.H. Orchard, Inhibition of spontaneous activity of rabbit atrioventricular node cells by KB-R7943 and inhibitors of sarcoplasmic reticulum Ca<sup>2+</sup> ATPase, *Cell Calcium* 49 (2011) 56–65.
- [26] A.E. Martynyuk, K.A. Kane, S.M. Cobbe, A.C. Rankin, Adenosine increases potassium conductance in isolated rabbit atrioventricular nodal myocytes, *Cardiovas. Res.* 30 (1995) 668–675.
- [27] A.J. Levi, J.C. Hancox, F.C. Howarth, J. Croker, J. Vinnicombe, A method for making rapid changes of superfusate whilst maintaining temperature at 37 °C, *Pflügers Arch.* 432 (1996) 930–937.
- [28] S. Dhein, C.J. van Koppen, O.E. Brodde, Muscarinic receptors in the mammalian heart, *Pharmacol. Res.* 44 (2001) 161–182.
- [29] M. Narita, Y. Furukawa, M. Takei, M. Murakami, L.M. Ren, Y. Karasawa, S. Chiba, Functional participation in M1 receptor subtype on chronotropic and dromotropic responses to vagus stimulation in anesthetized dogs, *J. Pharmacol. Exp. Ther.* 258 (1991) 166–170.
- [30] S.N. Hardouin, K.N. Richmond, A. Zimmerman, S.E. Hamilton, E.O. Feigl, N.M. Nathanson, Altered cardiovascular responses in mice lacking the M(1) muscarinic acetylcholine receptor, *J. Pharmacol. Exp. Ther.* 301 (2002) 129–137.
- [31] R.S. Alphin, J.R. Martens, D.M. Dennis, Frequency-dependent effects of propofol on atrioventricular nodal conduction in guinea pig isolated heart. Mechanism and potential antidysrhythmic properties, *Anesthesiology* 83 (1995) 382–394.
- [32] C.P. Bolter, D.J. English, The effects of tertiapin-Q on responses of the sinoatrial pacemaker of the guinea-pig heart to vagal nerve stimulation and muscarinic agonists, *Exp. Physiol.* 93 (2008) 53–63.
- [33] M. Yamada, The role of muscarinic K<sup>+</sup> channels in the negative chronotropic effect of a muscarinic agonist, *J. Pharmacol. Exp. Ther.* 300 (2002) 681–687.
- [34] K. Bender, M.C. Wellner-Kienitz, L.I. Bosche, A. Rinne, C. Beckmann, L. Pott, Acute desensitization of GIRK current in rat atrial myocytes is related to K<sup>+</sup> current flow, *J. Physiol.* 561 (2004) 471–483.
- [35] W.J. Zhang, X.J. Yu, H. Honio, M.S. Kirby, M.R. Boyett, On the role of G protein activation and phosphorylation in guinea-pig atrial cells, *J. Physiol.* 464 (1993) 649–679.
- [36] Y. Habuchi, M. Nishio, H. Tanaka, T. Yamamoto, L.L. Lu, M. Yoshimura, Regulation by acetylcholine of Ca<sup>2+</sup> current in rabbit atrioventricular node cells, *Am. J. Physiol.* 271 (1996) H2274–H2282.
- [37] Z. Shui, M.R. Boyett, W.J. Zhang, T. Haga, K. Kameyama, Receptor kinase-dependent desensitization of the muscarinic K<sup>+</sup> current in rat atrial cells, *J. Physiol.* 487 (1995) 359–366.
- [38] Z. Shui, I.A. Khan, H. Tsuga, T. Haga, M.R. Boyett, Role of receptor kinase in short term desensitization of cardiac muscarinic K<sup>+</sup> channels expressed in Chinese Hamster ovary cells, *J. Physiol.* 507 (1998) 325–334.
- [39] Z. Shui, I.A. Khan, T. Haga, J.L. Benovic, M.R. Boyett, Control of cardiac muscarinic K<sup>+</sup> channel by β-arrestin 2, *J. Biol. Chem.* (2001) 11691–11697.
- [40] T.T. Yamanushi, Z. Shui, R.N. Leach, H. Dobrzynski, T.W. Claydon, M.R. Boyett, Role of internalization of M2 muscarinic receptor via clathrin-coated vesicles in desensitization of the muscarinic K<sup>+</sup> current in heart, *Am. J. Physiol.* 292 (2006) H1737–H1746.
- [41] N.J. Freedman, A.S. Ament, M. Oppermann, R.H. Stoffel, S.T. Exum, R.J. Lefkowitz, Phosphorylation and desensitization of human endothelin A and B receptor. Evidence for G protein-coupled receptor kinase specificity, *J. Biol. Chem.* 272 (1997) 17734–17743.
- [42] G.E. Morris, C.P. Nelson, N.B. Standen, R.A. Challis, J.M. Willets, Endothelin signalling in arterial smooth muscle is tightly regulated by G protein coupled receptor kinase 2, *Cardiovasc. Res.* 85 (2010) 424–433.
- [43] M. Nishimura, R.M. Huan, Y. Habuchi, N. Homma, Y. Watanabe, Anticholinergic action of quinidine sulfate in the rabbit atrioventricular node, *Naunyn Schmiedeberg Arch. Pharmacol.* 341 (1990) 517–524.